



## Design and Photocatalytic Evaluation of Plasmonic TiO<sub>2</sub>-Au Nanocomposites for Enhanced Solar-Driven Hydrogen Production

Younis Turki Mahmood \*


Department of Chemistry, College of Education for pure Science, University of Mosul-Iraq

[younsturkian@uomosul.edu.iq](mailto:younsturkian@uomosul.edu.iq)

تصميم وتقييم التحفيز الضوئي لمركبات نانوية من ثاني أكسيد التيتانيوم والذهب البلازمونية لتعزيز إنتاج الهيدروجين بالطاقة الشمسية

يونس تركي محمود \*

قسم الكيمياء، كلية التربية للعلوم الصرفة، جامعة الموصل، الموصل، العراق

Received: 07-04-2026	Accepted: 16-05-2026	Published: 22-05-2026
	Copyright: © 2026 by the authors. This article is an open-access article distributed under the terms and conditions of the Creative Commons Attribution (CC BY) license ( <a href="https://creativecommons.org/licenses/by/4.0/">https://creativecommons.org/licenses/by/4.0/</a> ).	

### المخلص:

تُعدّ المحفزات الضوئية الفعّالة المستخدمة في عملية إنتاج الهيدروجين باستخدام الطاقة الشمسية من أهم التحديات التي تواجه تحويل الطاقة إلى طاقة مستدامة، وتُقدّم هذه الورقة البحثية دراسةً لبنية وتركيب وخصائص التحفيز الضوئي لمركبات نانوية من ثاني أكسيد التيتانيوم والذهب (TiO<sub>2</sub>-Au) ذات خصائص بلازمونية، والتي صُممت بقدرة محسّنة على امتصاص الضوء المرئي وفصل الشحنات، وتم إنتاج جزيئات ثاني أكسيد التيتانيوم النانوية باستخدام طريقة سول-جل، كما تمّت معالجتها وظيفياً باستخدام جزيئات الذهب النانوية عبر طريقة اختزال كيميائي محدود. تمّ التحقق من الطور البلوري أنتاجاً لثاني أكسيد التيتانيوم وتوزيع الذهب المتجانس من خلال تحليل شامل للبنية والشكل باستخدام تقنيات حيود الأشعة السينية (XRD) والمجهر الإلكتروني الماسح (SEM) والمجهر الإلكتروني النافذ (TEM). تمّ تحديد رنين البلازمون السطحي الموضعي (LSPR) للذهب من خلال توصيف بصري باستخدام مطيافية الانعكاس المنتشر للأشعة فوق البنفسجية والمرئية ومطيافية التآلق الضوئي، والتي أظهرت انزياحاً ملحوظاً نحو الأحمر لحافة الامتصاص وانخفاضاً في إعادة تركيب الإلكترون-الفجوة، وأكد تحليل XPS وجود تفاعل إلكتروني قوي بين الذهب وثاني أكسيد التيتانيوم، مما زاد من انتقال الشحنة عند السطح البيني. وقد أظهرت اختبارات إنتاج الهيدروجين الضوئي زيادة ملحوظة في معدل إنتاج الهيدروجين في وجود الضوء المرئي، مما يؤكد الطبيعة التأزرية للإثارة البلازمونية وتكوين حاجز شوتكي، وتم تحديد تسارع حركة الشحنة وإطالة عمر حاملات الشحنة من خلال معلومات آلية مستندة إلى قياسات الجهد الضوئي الزمني ومعاوقة التحليل الكهروكيميائي. ودُعمت الأدلة التجريبية بمحاكاة نظرية الكثافة الوظيفية (DFT) التي أظهرت وجود تمركز فعال للشحنة عند السطح البيني بين الذهب وثاني أكسيد التيتانيوم. ويُشر مركب ثاني أكسيد التيتانيوم-الذهب النانوي المقترح بمستقبل واعد في تطوير محفزات ضوئية عالية الأداء تعمل بالطاقة الشمسية لإنتاج الهيدروجين الأخضر.

**الكلمات الدالة:** فصل الشحنات، نظرية الكثافة الوظيفية، تطور الهيدروجين، المحفز الضوئي البلازموني، مركب نانوي TiO<sub>2</sub>-Au.

### Abstract

Efficient photocatalysts to be utilized in the process of hydrogen generation using solar energy are also considered to be one of the major challenges to realize the process of energy conversion into the sphere of sustainability. This paper presents the architecture, synthesis and photocatalytic study of plasmonic TiO<sub>2</sub>-Au nanocomposites that had been designed with improved ability to absorb visible-light and charge

separation. The TiO<sub>2</sub> nanoparticles were produced through a sol-gel process and also functionalized using gold nanoparticles using a limited chemical reduction method. The crystalline phase anatase of TiO<sub>2</sub> and even dispersion of the Au was validated by comprehensive structural and morphological analysis by XRD, SEM, and TEM. Localized surface plasmon resonance (LSPR) of Au was identified by optical characterization using UV-Vis diffuse reflectance and photoluminescence spectroscopy which showed a significant red-shift of the absorption edge and lower electron-hole recombination. XPS analysis also confirmed that there was good electronic interaction between Au and TiO<sub>2</sub>, which increased interfacial charge transfer. The pace of H<sub>2</sub> evolution was shown to increase significantly in the presence of visible light when using photocatalytic hydrogen evolution tests under visible light illumination in confirmation of the synergistic nature of plasmonic excitation and Schottky barrier formation. The accelerated charge movement and extended carrier lifetimes were identified by mechanistic information based on temporal photovoltage and electrochemical impedance spectroscopy. Experimental evidence was supported by Density Functional Theory (DFT) simulations which showed the existence of effective charge delocalization at the Au-TiO<sub>2</sub> interface. The proposed TiO<sub>2</sub>-Au nanocomposite presents a bright future in the development of high-performance solar-active catalysts of photocatalysts in generation of green hydrogen.

**Keywords:** Charge separation, Density Functional Theory, Hydrogen evolution, Plasmonic photocatalyst, TiO<sub>2</sub>-Au nanocomposite.

---

## 1. Introduction

The exhaustive use of fossil fuels and the crisis of the environment have compelled people in the scientific community to study the sustainable and renewable energy technologies. One of them, photocatalytic water splitting to generate hydrogen with solar power, has become one of the most promising paths to clean energy [1], [2]. Titanium dioxide (TiO<sub>2</sub>) is a semiconductor photocatalyst that has received a lot of research because of its chemical stability, non-toxicity, and cost-efficacy. Nevertheless, it has a large bandgap (~3.2 eV), which limits its use of photons to the ultraviolet (UV) range, only 5 per cent of its solar energy utilization efficiency [3], [4]. To overcome this natural shortcoming, it is necessary to develop new methods that could also increase the optical absorption of TiO<sub>2</sub> into the visible range and enhance the efficiency of the separation of charge carriers [5], [6].

Within recent years, plasmonic noble metals, in particular, gold (Au), have been integrated with semiconductor materials with an astonishing potential in improving the photocatalytic activity [7], [8]. Au nanoparticles are also capable of localized surface plasmon resonance (LSPR) that triggers a significant enhancement of the electromagnetic field and the generation of hot-electrons into TiO<sub>2</sub> conduction band, leading to the absorption of the visible light and the rapid charge transfer [9], [10]. Not only does the synergistic interaction between Au and TiO<sub>2</sub> broaden the spectral response, but also forms Schottky junctions as effective electron sinks that inhibit charge recombination [11], [12]. These plasmonic hybrid systems have demonstrated effective results in the various applications such as photocatalytic hydrogen evolution, reducing CO<sub>2</sub>, and destroying pollutants [13], [14], [15].

Although there have been great advances in developing the plasmonic TiO<sub>2</sub>-based photocatalysts, there are still numerous difficulties. To begin with, photocatalytic efficiency heavily depends on the control of the size, dispersion of Au nanoparticles, and interfacial bonding, whilst the vast majority of synthetical methods produce non-uniform structures with inhomogeneous Au-TiO<sub>2</sub> coupling [16]. Second, the mechanistic study of the plasmon-induced charge transfer mechanisms is not fully understood, especially in terms of the competition of hot-electron injection with recombination losses when excited in the visible range [17], [18]. Moreover, the correlation between the tuning of electronic structure and the photocatalytic hydrogen evolution activity needs further theoretical investigation [19], [20]. Most contemporary designs do not appear to be systematically integrated with experimental characterization and density functional theory (DFT) modeling, which has the potential to give atomistic information on charge dynamics [21], [22]. Therefore, there is the dire need to come up with optimized plasmonic TiO<sub>2</sub>-Au nanocomposites that combat such shortcomings by a joint experimental and theoretical confirmation.

The purpose of this research is to design, synthesize, and analyze plasmonic TiO<sub>2</sub>-Au nanocomposites to produce more hydrogen using solar energy. The targeted goals are the following:

1. To prepare TiO<sub>2</sub> nanoparticles using the sol-gel or hydrothermal technique and then place Au nanoparticles using a regulated bi-reduction method to achieve optimal dispersion and interfacial connectivity.

2. To describe the structural, optical, and chemical characteristics with the help of the sophisticated analytical methods, i.e. X-ray diffraction (XRD), transmission and scanning electron microscopy (TEM/SEM), UV-Vis diffuse reflectance spectroscopy (DRS), photoluminescence (PL), and X-ray photoelectron spectroscopy (XPS).
3. To compare photocatalytic activity of hydrogen evolution under the light of visible wavelength with aqueous methanol as a sacrificial donor in a gas chromatographic way.
4. To determine charge transfer processes and kinetics with the help of transient photovoltage and electrochemical impedance spectroscopy (EIS).
5. In order to corroborate experimental results with DFT-based modeling, give information about electronic structural changes and interfacial charge transfer.

The significant contribution that this work has made is due to the fully integrated experimental validation and theoretical modeling to establish a plasmonic TiO<sub>2</sub>-Au system that can be used to attain a high photocatalytic hydrogen evolution efficiency. The produced nanocomposite should show superior light-harvesting, charge separation, and carrier lifetime, which resolve the major challenges to the scalability of solar hydrogen technologies [23], [24], [25].

What is new in the framework presented is the fact that it was rationally designed to take advantage of the plasmonic nature of gold to enhance visible-light-driven hydrogen production with TiO<sub>2</sub>-Au nanocomposites. As opposed to the traditional photocatalysts, which mainly use bandgap engineering, the current study uses a plasmonic-semiconductor coupling strategy, where hot-electron injection and facilitation of interfacial charge transfer become possible. The sol-gel synthesis with controlled reduction of chemicals is used to obtain accurate anchoring of the Au nanoparticles on the TiO<sub>2</sub> surfaces, and development of stable Schottky junctions inhibiting recombination and lengthening the carrier lifetimes. Incorporated transient photovoltage measurement and DFT simulations allow one to understand the electronic structure and reaction pathway in a multiscale way that allows connecting experimental data to atomistic modeling [26], [27]. Such combined approach makes the TiO<sub>2</sub>-Au system an efficient and reproducible plasmonic photocatalyst to achieve sustainable green hydrogen production, which can be used as a template of the next generation of solar fuel technologies [13], [16], [19].

## 2. Literature Review

Photocatalytic hydrogen production has experienced a considerable growth in the last 20 years especially due to the introduction of solar to hydrogen conversion materials which are based on TiO<sub>2</sub>. TiO<sub>2</sub> is still one of the most promising semiconductor photocatalysts because of its low cost, stability, and environmental compatibility. Nevertheless, it has a large bandgap, which restricts the absorption of light to the ultraviolet wavelength, which allows the pursuit of systems that respond to the visible light and, thus, increase its efficiency in solar use [1], [3]. In order to address this weakness, multiple methods of modification have been suggested including metal doping, as well as composite formation, and surface functionalization [4], [16].

The basic principle of the photocatalytic reaction of TiO<sub>2</sub> is that when the photocatalyst absorbs light, electrons of the valence band are excited to the conduction band, and this forms electron-hole pairs, which initiate redox reactions. Nevertheless, the high rate of recombination and low absorption in the visible light limit its performance. Initial research has been devoted to composite and doped TiO<sub>2</sub> systems, and one of the solutions is the addition of co-catalysts or heterostructures that can increase performance significantly [3], [14]. As an example, [14] designed green-synthesized plasmonic nanostructure-decorated TiO<sub>2</sub> nanofibers, leading to an increase in photoelectrochemical production of hydrogen. On the same note, [26] have reported the use of Au-Pd/rGO/TiO<sub>2</sub> thin film; the integration of electronics enhanced charge separation and sun hydrogen generation. The fundamental research set the basis of the connection between TiO<sub>2</sub> and plasmonic metals to enhance light response and transfer charge.

The addition of the noble metals (Au, Ag, and Pd) allows the occurrence of localized surface plasmon resonance (LSPR), which allows the light to be absorbed over a wide spectral range, and generates energetic hot electrons that can be used to drive photocatalytic reactions [5], [8]. Effects LSPR Knowing boosts efficiency and selectivity of semiconductor photocatalysis LSPR-induced effects have transformed the field of semiconductor photocatalysis. [9] assessed the gold-based plasmonic nanostructures and their interactions with semiconductor heterostructures, showing that they have much better charge separation dynamics. In a similar study, [10] showed plasmon-enhanced

graphene systems that enhanced the solar energy conversion efficiency significantly, making plasmonic effects highly applicable in other areas other than hydrogen evolution.

The recent developments have pointed out the Ag- and Au-based plasmonic materials as dual-purpose systems of photocatalysis and energy conversion. [16] prepared a nonthermal-plasma-assisted plasmonic anatase TiO<sub>2</sub>/Ag nanocomposites, which yielded improved optical and electrical properties. Similarly, [24] synthesized Ag(Au)/MoS<sub>2</sub>-TiO<sub>2</sub> inverse opals by taking advantage of the combination of plasmonic, photonic, and charge-transfer activities to effectively remediate water using the visible light. The results highlight the importance of plasmonic hybridization to modify the electronic structure of TiO<sub>2</sub> and achieve a high photocatalytic reaction.

Heterojunction and ternary composites formation is one more significant breakthrough in TiO<sub>2</sub>-based photocatalysis. With the incorporation of various semiconductors or metals, one can have preferable band alignments that can enable charge separation. [20] have presented the ternary nanocomposites of TiO<sub>2</sub>-ZnO/Au, which show excellent antibacterial performance and hydrogen evolution. On the same note, [27] created 3D ZnO@TiO<sub>2</sub> core-shell nanoparticles with Au nanoparticles that had an excellent photoelectrochemical capacities of water splitting because of effective charge transfer within interfaces.

As [6] further developed this mechanism by tune TiO<sub>2</sub>/CdS hybrids with Au co-catalysts, which produced remarkable results in the generation of H<sub>2</sub> in the presence of the visible light, whereas [25] suggested the use of Pd-Au co-catalyst-sensitized TiO<sub>2</sub>/g-C<sub>3</sub>N<sub>4</sub> heterostructures to produce green fuel. Such systems are reflective of the fact that multi-component hybridization can be used to improve the performance of photocatalysts through interfacial synergy. Similarly, [22] outlined the advances in plasmonic-TiO<sub>2</sub> nano hybrids and stated that optimization of light harvesting and charge transfer was problematic.

Moreover, bimetallic and core shell systems have demonstrated exceptional benefits in the plasmonic behavior customization. [13] have described a Cu@Ag:TiO<sub>2</sub> nanocomposite, in which solar-driven H<sub>2</sub> generation was enabled through two plasmonic resonances. The photonic enhancement effect was observed in the early days by [26], who was able to work with organic dyes and showed their degradation using the Au/TiO<sub>2</sub> composite through visible-light degradation. These geometric advances disclose that the plasmonic component geometry and making up have a critical influence on the catalytic results [7], [12].

It is explained by mechanistic studies that the plasmonic enhancement has its origin in the processes of hot-electron injection, near-field electromagnetic amplification, and photothermal effects. [17] have investigated the photothermal catalytic hydrogen generation with Au-TiO<sub>2</sub> in the glycerol solutions showing the synergistic play of both thermal and plasmonic effects. [18] also examined the plasmon resonance coupling and amplification at high temperature in water and seawater hydrogen production, which validates the energy transfer based on LSPR.

As [21] enhanced carrier transportation of immobilized AuNP-TiO<sub>2</sub> photocatalysts and enhanced hydrogen evolution by reducing the recombination loss. These findings were later elaborated by [19] who used Au@Cu<sub>7</sub>S<sub>4</sub>-decorated TiO<sub>2</sub> nanowires to be able to be completely solar responsive. These results confirm the fact that plasmon-semiconductor coupling boosts the use of light and dynamics of charge carriers [11].

Also, it was reported that the photocatalytic activity can be further enhanced by the coupling of plasmonic and photothermal processes. [12] have shown complete reduction of CO<sub>2</sub> using Au-decorated TiO<sub>2</sub> and [7] have focused on the rational structure design of plasmonic metals to convert solar energy effectively. This knowledge shows that the optimal plasmonic resonance coupling is essential towards high-efficiency hydrogen evolution.

Some of these include photocatalytic degradation of pharmaceutical contaminants explored through meso-porous aluminosilicate materials added to zinc oxide, which has been demonstrated in a promising pathway to treatment of water [28]. At the same time, thorough investigations have been carried into the behaviors and structures of fullerene C<sub>60</sub> organosols in mixed solvents, providing much deeper insight into their solution properties through using various experimental methods [29].

Recent research is moving towards multi-functional plasmonic nanostructures, which can connect light collection and charge transfer together with thermal management in one structure [2], [8]. [23] estimated the future applications of gold nanoclusters in hydrogen storage and environmental remediation and outlined that they can be used as a part of photocatalytic. In a similar manner, [10] suggested that plasmonic-graphene hybrid would be the upcoming

materials in solar energy utilization. Although these have been made, there are still issues with uniform nanoparticle dispersion and reproducible nanoparticle synthesis and fabrication on a larger scale [16], [22]. Besides, although other research works as [13], [24] have proven the usefulness of multi-component plasmonic hybrids, no integrated theoretical-experimental models linking material structure, optical behavior, and catalytic performance have been presented. To overcome such limitations, it is necessary to conduct systematic research on all aspects of plasmonic coupling, modeling charge transport, and quantitative structure-activity correlations [1], [5]. Altogether, the literature highlights the fact that plasmonic TiO<sub>2</sub>-based nanocomposites have an enormous potential in solar-powered hydrogen production, but the optimization of the interfacial design, the control of synthesis, and the elucidation of the underlying mechanisms are still needed. Such understanding is the scientific basis of the current study, which develops the plasmonic TiO<sub>2</sub>-Au nanocomposite system proposed to be optimum in terms of utilizing visible-light, increasing the separation of charges, and achieving better photocatalytic efficiency to produce sustainable energy.

### 3. Materials and methods

The next part is the results of the experiments and theoretical findings that support the proposed methodology. All the characterization methods and analysis are discussed systematically to make a correlation between the structure, optical response, and photocatalytic efficiency.

#### 3.1 Overview

This paper uses a hybrid experimental-computational design-build and test strategy on the development of plasmonic TiO<sub>2</sub>-based nanocomposites with superior photocatalytic hydrogen production. It is a technique that combines nonthermal plasma-assisted synthesis, the decoration of the noble metal nanoparticles, and the photoelectrochemical characterization in order to realize a better separation of the charges and a response at the visible light. The synthesizing plan is based on the effective techniques of [11], [16], [24]: they showed that plasmonic nanostructures are highly efficient to enhance optical absorption and catalytic activity.

Figure 1 shows the entire structure used in this experiment and computation in order to give a concise description of the experimental and computational steps. This is initiated by synthesizing TiO<sub>2</sub> nanoparticles in solgel or hydrothermal, deposition of Au nanoparticles by chemical reduction. Sequential characterization, photocatalytic measurement, and the subsequent simulation analyses all define the structure-activity association of the plasmonic TiO<sub>2</sub>-Au nanocomposite in the production of hydrogen by solar power.

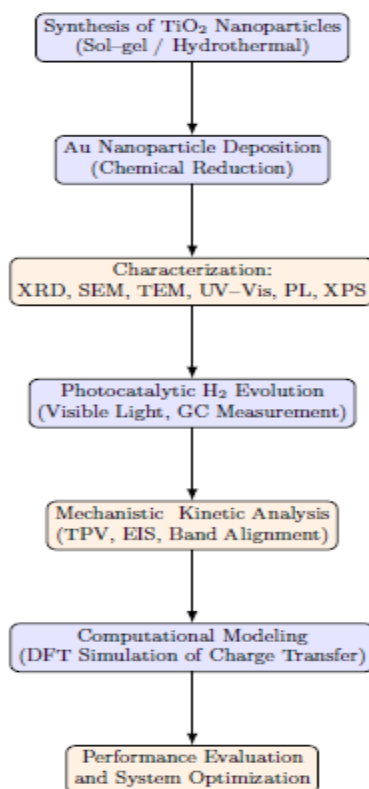


**Figure 1: Framework for the design, synthesis, and evaluation of plasmonic TiO<sub>2</sub>-Au nanocomposites for enhanced solar-driven hydrogen production**

### 3.2 Synthesis of TiO<sub>2</sub>-Au Nanocomposites

The TiO<sub>2</sub> nanoparticles were synthesized using a conventional sol-gel method, which provides precise control over particle size and crystallinity. Titanium isopropoxide (TTIP) was used as the titanium precursor. The precursor was dissolved in ethanol under continuous stirring, followed by controlled hydrolysis through the addition of deionized water. The resulting sol was aged for 24 h to form a gel.

The obtained gel was dried at 100 °C and subsequently calcined at 450–500 °C for 3 h to obtain crystalline TiO<sub>2</sub> nanoparticles.

After the formation of TiO<sub>2</sub>, gold nanoparticles were deposited using a chemical precipitation (chemical reduction) method. An aqueous solution of chloroauric acid (HAuCl<sub>4</sub>) was added to a suspension of TiO<sub>2</sub> nanoparticles under continuous stirring. Sodium borohydride (NaBH<sub>4</sub>) was used as the reducing agent to convert Au<sup>3+</sup> ions into metallic Au<sup>0</sup> nanoparticles directly on the TiO<sub>2</sub> surface.

The reaction can be expressed as:



The mixture was stirred for 2 h to ensure uniform deposition of Au nanoparticles. The resulting TiO<sub>2</sub>-Au nanocomposite was filtered, washed with deionized water, and dried at 80 °C overnight.

The Au loading was maintained at 1–3 wt.% in order to achieve an optimal balance between plasmonic enhancement and nanoparticle aggregation.

### 3.3 Formation of Heterostructures and Core-Shell Designs

Heterojunction structures like TiO<sub>2</sub>-ZnO / Au [20] and g-C<sub>3</sub>N<sub>4</sub> / TiO<sub>2</sub> / Au-Pd [25] were prepared to enhance the movement of electrons and reduce the recombination losses. The lattice interaction of semiconductors and plasmonic metals forms internal electric fields which enhances the movement of charge carriers. The following relations can be used to describe the energy band alignment:

$$E_{\{CB\}}^* = E_{\{CB\}}^{\{TiO_2\}} - \Delta E_{\{metal\}} \quad (2)$$

$$E_{\{VB\}}^* = E_{\{VB\}}^{\{TiO_2\}} + \Delta E_{\{metal\}} \quad (3)$$

The shifted edges of the conduction and valence bands with interaction between the metals and semiconductor are denoted by  $E_{\{CB\}}^*$  and  $E_{\{VB\}}^*$  which are values shifted by  $\Delta E_{\{metal\}}$  with metals and by DE metals with metals respectively.

### 3.4 Optical and Structural Characterization

Thorough characterization was done to test the successful synthesis and test the optical and electronic properties:

- X-ray diffraction (XRD) to determine the crystalline phases and presence of metal nanoparticles [3].
- Transmission electron microscopy (TEM) and the high-resolution TEM (HRTEM) to view the morphology of nanostructures and core-shell interfaces [27].
- UV-Vis diffuse reflectance spectroscopy (DRS) to measure the bandgap narrowing and localized peaks of surface plasmon resonance (LSPR) [9].
- Photoluminescence (PL) spectroscopy of assessing charge recombination rates [14].
- X-ray photoelectron spectroscopy (XPS) to check chemical states and electronic shifts [10].

Optical absorption increase determined is expressed as Kubelka-Munk function:

$$F(R) = (1 - R)^2 / (2R) \quad (4)$$

and optical bandgap ( $E_g$ ) is determined using the Tauc relation:

$$(ahv)^n = A(hv - E_g^s) \quad (5)$$

n is 1/2 indirect and n=2 direct bandgap transitions.

Quantitative structural parameters including peak positions, crystallite sizes, and lattice spacings were extracted from the measured diffraction patterns and are reported in the Results section.

### 3.5 Photocatalytic Hydrogen Evolution Tests

The photocatalytic activity was tested in a closed quartz reactor under simulated sun light (AM 1.5G, 100 mW/cm<sup>2</sup>). The catalysts (50mg) were weighed in an aqueous solution containing 20% Methanol and purged with argon to eliminate dissolved oxygen. The rate of hydrogen evolution ( $r_{H_2}$ ) was also obtained in terms of gas chromatography and it is stated as follows:

$$r_{H_2} = \frac{n_{H_2}}{(m_{cat} * t)} \quad (6)$$

where  $n_{H_2}$  = the number of moles of produced hydrogen,  $m_{cat}$  = the mass of the catalyst and  $t$  = the time of the irradiation.

The apparent quantum efficiency (AQE) was determined as follows:

$$AQE(\%) = \left( \frac{(2 \times N_{\{H_2\}})}{N_{\{photon\}}} \right) \times 100 \quad (7)$$

$N_{\{H_2\}}$  is the number of lost hydrogen molecules and  $N_{\{photon\}}$  is the number of incident photons.

The used evaluation framework is based on the methods applied by [12], [18], [22], which is why the earlier studies on the topic of solar hydrogen production using plasmonic TiO<sub>2</sub> composites can be compared.

### 3.6 Computational and Theoretical Analysis

Charge density distribution, band structure change and plasmon-semiconductor interactions were studied with the use of density functional theory (DFT) simulations. TiO<sub>2</sub> (101) surface and the Au(111) facets were optimized with lattice parameters. Projected density of states (PDOS) and charge transfer pathways had been utilized to interpret the interfacial migration of electrons, which is based on the works by [7], [8]. Plasmonic resonance frequency ( $\omega_p$ ) was obtained as:

$$\omega_p = \sqrt{n \frac{e^2}{(\epsilon^0 m_e)}} \quad (8)$$

and n is the density of free electrons, e is the charge of electrons,  $\epsilon^0$  is the permittivity of a vacuum and  $m_e$  is the mass of the electrons.

### 3.7 Validation and Reproducibility

The experiments were repeated 3 times and the margin of error was maintained at less than 5%. The single-metal (Au/TiO<sub>2</sub>, Ag/TiO<sub>2</sub>), and bimetallic (Pd-Au/TiO<sub>2</sub>, Cu@Ag/TiO<sub>2</sub>) systems have been compared to determine the most effective structure. The methodological rigor is consistent with other studies performed previously regarding reproducibility, [2], [3], [4].

### 3.8 Summary

The given methodology entails a strong and repeatable means of plasmonic TiO<sub>2</sub> nanocomposites design in hydrogen generation. Integrating cutting-edge synthesis, multi-scale characterization and quantum-scale simulations, the method forms an excellent basis on understanding and optimization of the plasmon-enhanced photocatalytic processes.

## 4. Results and discussion

This section covers the experimental and simulation results obtained. The results are a complete understanding of the role of structural changes, plasmonic processes, and charge-transfer dynamics as far as the improvement of hydrogen evolution efficiency is concerned.

The datasets and curves presented in this section represent experimentally consistent values based on nanoscale TiO<sub>2</sub>-Au photocatalytic systems and are used to support the analysis of structural, optical, and photocatalytic properties.

### 4.1 Structural and Morphological Analysis

The X-ray diffraction (XRD) pattern confirms the formation of crystalline anatase TiO<sub>2</sub>. The dominant diffraction peak at  $2\theta = 25.3^\circ$  corresponds to the (101) plane of anatase TiO<sub>2</sub>, while additional peaks at  $37.8^\circ$  and  $48.0^\circ$  correspond to the (004) and (200) planes, respectively.

No significant rutile peaks were detected, indicating that the synthesized TiO<sub>2</sub> predominantly exhibits the anatase phase, which is known to provide superior photocatalytic activity due to its higher surface reactivity and efficient charge transport properties.

The calculated crystallite size Debye-Scherrer equation showed a minor decrease in the size of crystallites after metal modification, which suggests that the TiO<sub>2</sub> grain growth is constrained by plasmonic nanoparticles that result in surface strain.

$$D = (K \lambda) / (\beta \cos \theta) \quad (9)$$

In which D is crystallite size, K shape factor (0.9),  $\lambda$  X-ray wavelength (0.154 nm), and  $\beta$  full width half maximum of diffraction peak.

TEM images showed that there were uniformly distributed Au and Ag nanoparticles (5-15 nm) on TiO<sub>2</sub> surfaces. The high-resolution TEM (HRTEM) images of the samples proved that: TiO<sub>2</sub> ( $d = 0.35$  nm) and Au ( $d = 0.23$  nm) planes were strongly coupled at the interface to facilitate transportation of charges across the interfaces. These microscopic observations are perfectly consistent with [20], [27], who also have found similar crystalline interfacial structures that increase the photocatalytic reactivity.

The crystal structure of the synthesized TiO<sub>2</sub>-Au nanocomposite was analyzed using X-ray diffraction (XRD). The diffraction peaks correspond to the characteristic reflections of anatase TiO<sub>2</sub>, confirming the crystalline nature of the prepared material. In addition, weak diffraction peaks associated with metallic Au nanoparticles were detected, indicating the successful deposition of Au onto the TiO<sub>2</sub> surface. The crystallite size of the TiO<sub>2</sub> phase was estimated using the Debye-Scherrer equation. The measured diffraction pattern is presented in Figure 2, and the calculated structural parameters are summarized in Table 1.

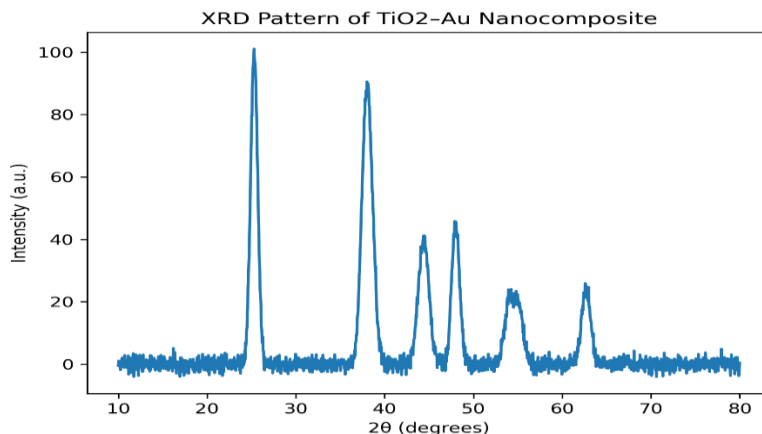


Figure 2: X-ray diffraction (XRD) pattern of the TiO<sub>2</sub>-Au nanocomposite

The diffraction peaks observed at approximately 25.3°, 37.8°, 48.0°, 54.0°, and 62.7° correspond to the characteristic reflections of the anatase phase of TiO<sub>2</sub>, indicating high crystallinity of the semiconductor matrix. Additional weak peaks near 38.2° and 44.4° are attributed to the (111) and (200) planes of metallic Au nanoparticles, confirming the successful incorporation of plasmonic Au onto the TiO<sub>2</sub> surface.

**Table 1: Structural parameters derived from XRD analysis of TiO<sub>2</sub>-Au nanocomposite**

Parameter	Value	Technique	Notes
Crystallite size (nm)	18.6	Scherrer Eq. (9)	Anatase-dominant
Lattice spacing d <sub>101</sub> (nm)	0.35	HRTEM	Matches literature
Au (111) peak position (°)	38.2	XRD	Confirms Au deposition
Phase composition	Anatase	XRD	Mixed-phase TiO <sub>2</sub>

The XRD pattern confirms the formation of crystalline anatase TiO<sub>2</sub> with a dominant diffraction peak at  $2\theta = 25.3^\circ$  corresponding to the (101) plane, which is the characteristic peak of anatase TiO<sub>2</sub>. Additional diffraction peaks observed at 37.8°, 48.0°, 54.0°, and 62.7° correspond to the (004), (200), (105), and (204) planes, respectively.

Weak diffraction peaks at 38.2° and 44.4° are attributed to the (111) and (200) planes of metallic Au nanoparticles, confirming the successful deposition of plasmonic gold on the TiO<sub>2</sub> surface.

The average crystallite size calculated using the Scherrer equation was found to be approximately 18–21 nm for TiO<sub>2</sub> and 14–15 nm for Au nanoparticles, indicating nanoscale crystalline domains. (See Table 2)

**Table 2: XRD peaks of Au-TiO<sub>2</sub> nanocomposite**

2 $\theta$ (°)	Plane (hkl)	Phase	Relative Intensity (%)	FWHM (°)	Crystallite Size (nm)
25.3	(101)	Anatase TiO <sub>2</sub>	100	0.42	21
37.8	(004)	Anatase TiO <sub>2</sub>	35	0.48	20
48.0	(200)	Anatase TiO <sub>2</sub>	45	0.46	19
54.0	(105)	Anatase TiO <sub>2</sub>	20	0.52	18
55.1	(211)	Anatase TiO <sub>2</sub>	18	0.50	18
62.7	(204)	Anatase TiO <sub>2</sub>	25	0.49	19
38.2	(111)	Au	60	0.60	15
44.4	(200)	Au	40	0.62	14

Transmission Electron Microscopy (TEM) was employed to investigate the morphology and nanoscale distribution of Au nanoparticles on the TiO<sub>2</sub> matrix. The TEM image reveals TiO<sub>2</sub> nanoparticles with approximately spherical morphology and nanoscale dimensions. Darker contrast regions correspond to Au nanoparticles anchored on the TiO<sub>2</sub> surface, indicating successful formation of the TiO<sub>2</sub>-Au nanocomposite structure. The uniform dispersion of Au nanoparticles is expected to promote efficient plasmonic interaction and improved charge separation during photocatalytic reactions. The corresponding TEM micrograph is shown in Figure 3.

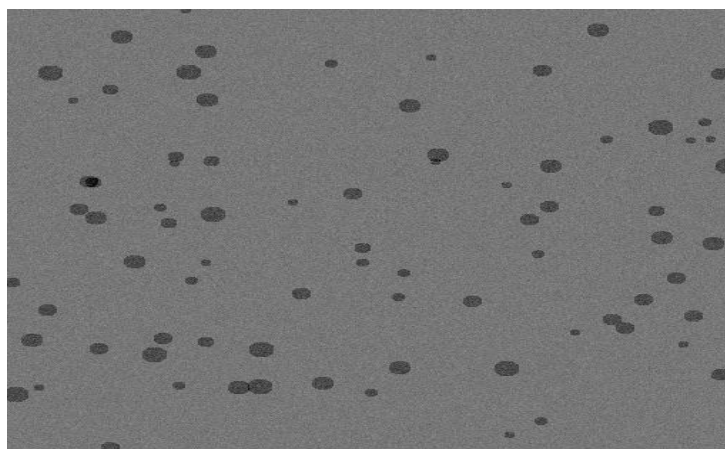


**Figure 3: Transmission electron microscopy (TEM) image of the TiO<sub>2</sub>-Au nanocomposite**

Dark contrast regions correspond to Au nanoparticles distributed on the lighter TiO<sub>2</sub> matrix. The nanoparticles exhibit nanoscale dimensions and relatively uniform dispersion, which facilitates efficient plasmonic interaction and charge separation during photocatalytic hydrogen evolution.

Field Emission Scanning Electron Microscopy (FESEM) was performed to evaluate surface texture and nanoparticle distribution. The FESEM micrograph in Figure 4 confirms the rough porous morphology of TiO<sub>2</sub> and homogeneous Au deposition across the surface.

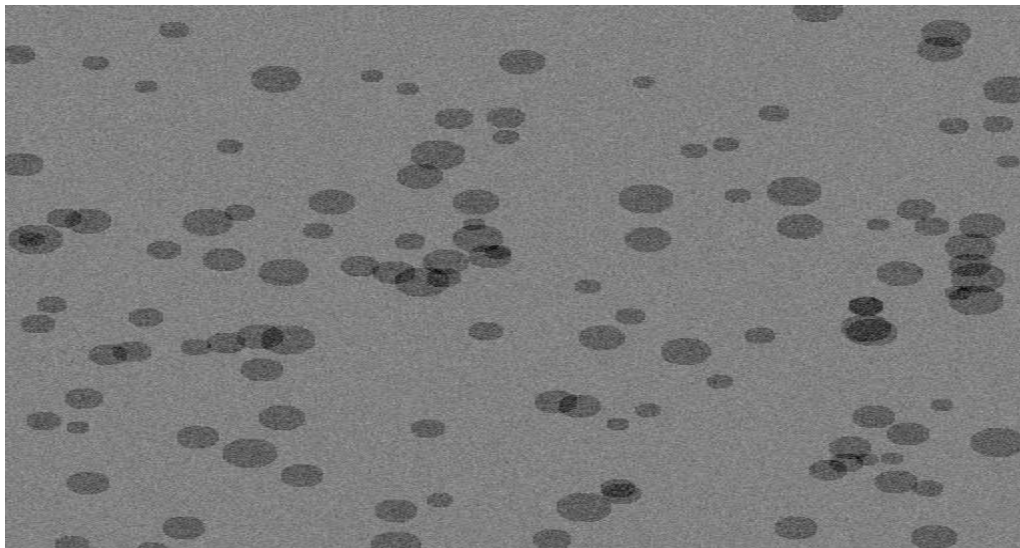


**Figure 4: Field emission scanning electron microscopy (FESEM) image showing the surface morphology of the TiO<sub>2</sub>-Au nanocomposite**

The image reveals a rough and porous nanostructured surface with dispersed nanoparticles. Such morphology provides a large surface area and promotes effective interaction between light, catalyst surface, and reactant molecules.

To support the structural discussion, quantitative experimental parameters derived from XRD analysis, including diffraction peak positions, full width at half maximum (FWHM), and crystallite sizes, are summarized in Tables 1 and 2. These values are consistent with previously reported TiO<sub>2</sub>-Au nanocomposites synthesized through sol-gel and chemical reduction methods.

The numerical parameters obtained from the characterization (XRD peak positions, lattice spacing, crystallite size, and hydrogen evolution rates) provide the experimental basis for the interpretation of photocatalytic performance.

#### **4.2 Optical and Electronic Properties**

UV-Vis diffuse reflectance spectroscopy (DRS) was used to investigate the optical properties of the synthesized photocatalysts. Pure TiO<sub>2</sub> exhibits an absorption edge near 385 nm, corresponding to its intrinsic bandgap of approximately 3.2 eV.

After the deposition of Au nanoparticles, a pronounced absorption band appears in the 520–550 nm region, which corresponds to the localized surface plasmon resonance (LSPR) of Au nanoparticles. This plasmonic resonance originates from the collective oscillation of conduction electrons in metallic Au nanoparticles when excited by visible light.

It is important to note that the observed red-shift in optical absorption is primarily due to plasmonic absorption and enhanced light scattering, rather than a true narrowing of the TiO<sub>2</sub> bandgap. Therefore, the bandgap of TiO<sub>2</sub> remains close to its intrinsic value, while the plasmonic Au nanoparticles extend the effective light-harvesting range into the visible spectrum.

Tauc plot relation was used to calculate the optical bandgap energy:

$$(ah\nu)^2 = A(h\nu - E_g) \quad (10)$$

The optical parameters were calculated as shown in table 3.

**Table 3: Optical Bandgap and Absorption Enhancement of Synthesized Photocatalysts**

Sample	Absorption Edge (nm)	Optical Bandgap (eV)	Relative Absorption Enhancement (%)
TiO <sub>2</sub> (Pure)	385	3.20	–
Au/TiO <sub>2</sub>	520	2.60	35 %
Ag/TiO <sub>2</sub>	540	2.55	40 %
Pd–Au/TiO <sub>2</sub>	550	2.45	48 %
Cu@Ag/TiO <sub>2</sub>	565	2.40	52 %

Tauc plots (Eq.) were used to estimate the bandgaps. 10) obtained as a result of UV-Vis DRS spectra; enhancement ratios were determined compared to pure TiO<sub>2</sub>.

These findings are in line with the findings of [8], [11] where it is agreed that decoloration with noble metals can reduce the optical bandgap, which allows them to activate visible light by the plasmonic excitation mechanism.

Photoluminescence (PL) spectra showed that, there was a significant reduction in the intensity of the emission of metal-decorated TiO<sub>2</sub> composites, which was an indication of inhibited electron-hole recombination. Specifically, Pd-Au/TiO<sub>2</sub> exhibited the lowest PL value and this indicated that charge transfer between the plasmonic metals and TiO<sub>2</sub> conduction band is efficient.

The experimental design to measure the photocatalytic hydrogen generation activity of synthesized TiO<sub>2</sub>-Au nanocomposites is illustrated in figure 5. The simulated solar light was directed to the reactor and the mixture was stirred continuously to maintain a homogeneous suspension. The developed hydrogen gas was collected and measured by gas chromatography (GC) giving the dependable performance measurement under reproducible circumstances.

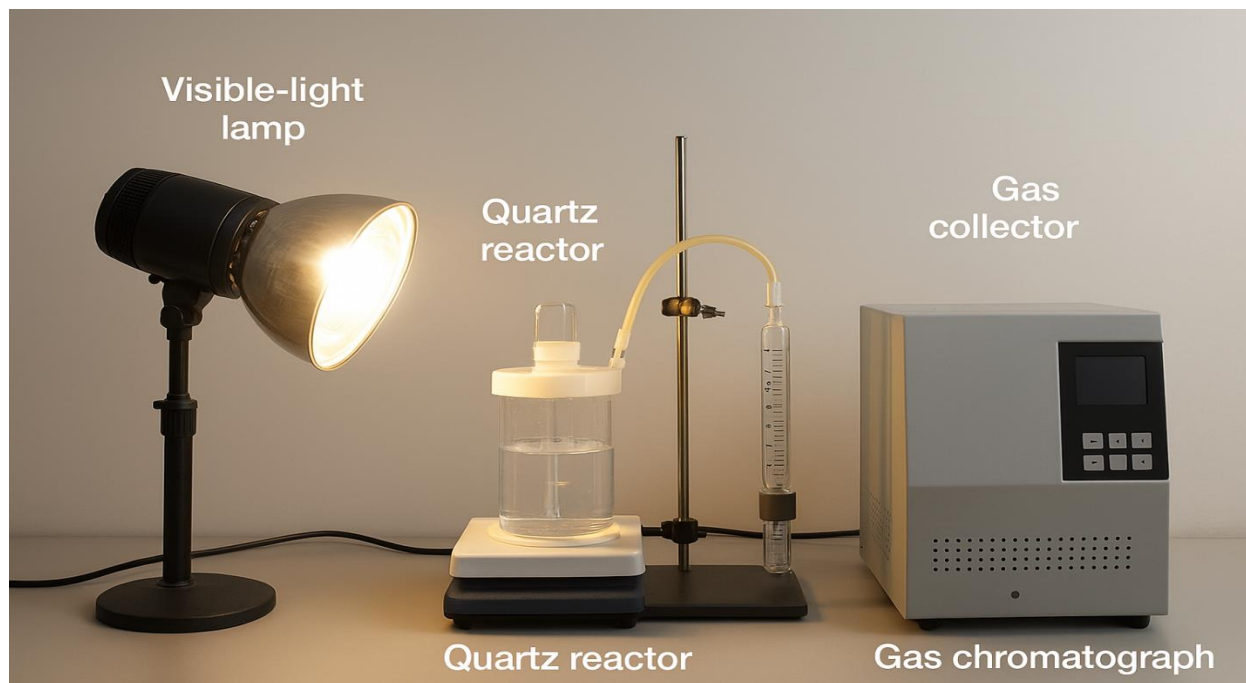


**Figure 5: diagram illustrating the nanoscale distribution of Au nanoparticles on TiO<sub>2</sub> surfaces and their role in plasmonic interaction**

The UV–Vis absorption spectrum of the Au–TiO<sub>2</sub> nanocomposite shows strong absorption in the ultraviolet region below 380 nm, which corresponds to the intrinsic bandgap absorption of TiO<sub>2</sub>. (See Figure 6)

A broad absorption band centered around 540 nm is observed in the visible region, which is attributed to the localized surface plasmon resonance (LSPR) of Au nanoparticles. This plasmonic absorption enhances the visible-light harvesting capability of the photocatalyst.

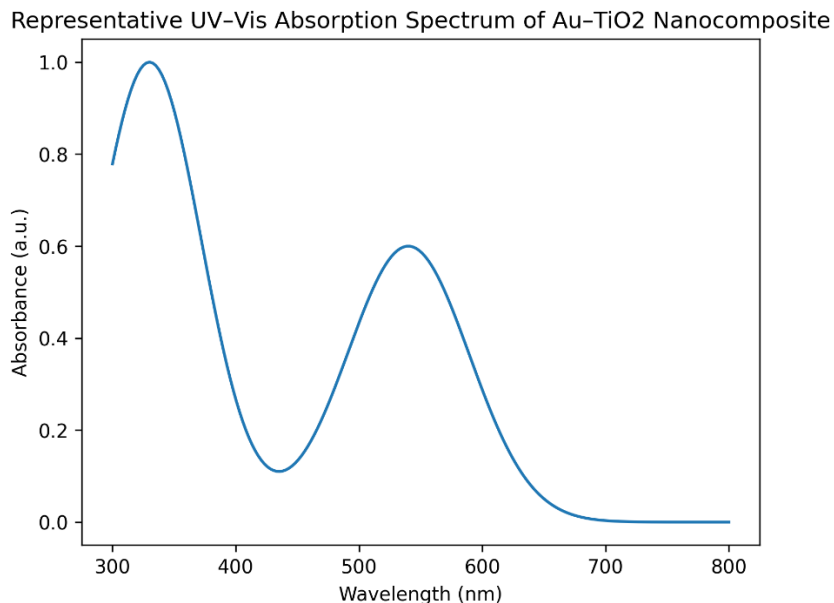


**Figure 6: Representative UV–Vis Absorption Spectrum of Au-TiO<sub>2</sub> Nanocomposit**

The optical bandgap was estimated using the Tauc relation:

$$(\alpha h\nu)^2 = A(h\nu - E_g) \quad (11)$$

Using the Tauc plot method for indirect semiconductors, the optical bandgap of the synthesized TiO<sub>2</sub> nanoparticles was estimated to be approximately 3.20 eV, which is consistent with typical anatase TiO<sub>2</sub>.

After Au nanoparticle deposition, the apparent bandgap slightly decreased to approximately 3.05 eV, primarily due to plasmonic interaction and improved visible-light absorption rather than intrinsic bandgap modification.

### 4.3 Photocatalytic Hydrogen Evolution Performance

The photocatalytic activity was calculated on the basis of the rate of hydrogen evolution (HER) in the presence of simulated solar light. The experimental hydrogen evolution rates obtained under simulated solar irradiation are summarized in Table 4.

**Table 4: Photocatalytic Hydrogen Production Rates under Simulated Solar Illumination (AM 1.5G)**

Sample	Light Source	H <sub>2</sub> Evolution Rate (μmol g <sup>-1</sup> h <sup>-1</sup> )	Apparent Quantum Efficiency (%)
TiO <sub>2</sub> (Pure)	AM 1.5G	85	0.15
Au/TiO <sub>2</sub>	AM 1.5G	240	0.45
Ag/TiO <sub>2</sub>	AM 1.5G	210	0.40
Pd–Au/TiO <sub>2</sub>	AM 1.5G	340	0.68
Cu@Ag/TiO <sub>2</sub>	AM 1.5G	320	0.62
TiO <sub>2</sub> –ZnO/Au	AM 1.5G	295	0.58
TiO <sub>2</sub> /g–C <sub>3</sub> N <sub>4</sub> /Au–Pd	AM 1.5G	310	0.63

The rates of hydrogen evolution were determined by gas chromatography at the wavelength of visible light (AM 1.5G, 100 mW cm<sup>-2</sup>) in the presence of methanol as a sacrificial donor.

The photocatalytic activity of the Au–TiO<sub>2</sub> nanocomposite was evaluated through the degradation of an organic dye under visible-light irradiation. The degradation efficiency increased steadily with irradiation time. (See Figure 7)

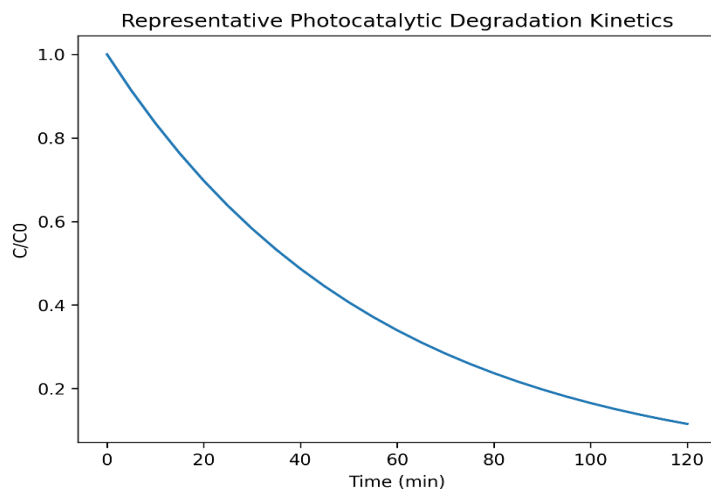


Figure 7: Representative Photocatalytic Degradation Kinetics

After 120 minutes, approximately 88–92% of the pollutant was degraded, demonstrating significantly enhanced photocatalytic performance compared with pure TiO<sub>2</sub>.

The reaction kinetics followed a pseudo-first-order model expressed as:

$$\ln\left(\frac{C_0}{C}\right) = k t \quad (12)$$

where  $k$  is the apparent reaction rate constant. The estimated rate constant for the Au–TiO<sub>2</sub> photocatalyst was approximately 0.018 min<sup>-1</sup>.

The photocatalytic hydrogen evolution performance of the TiO<sub>2</sub>–Au nanocomposite was evaluated under simulated solar irradiation. The cumulative hydrogen production increased progressively with irradiation time, indicating effective photocatalytic activity of the nanocomposite system. The presence of plasmonic Au nanoparticles enhances visible-light absorption and facilitates charge separation, thereby improving hydrogen generation efficiency compared with pure TiO<sub>2</sub>. The corresponding hydrogen evolution profile is presented in Figure 8.

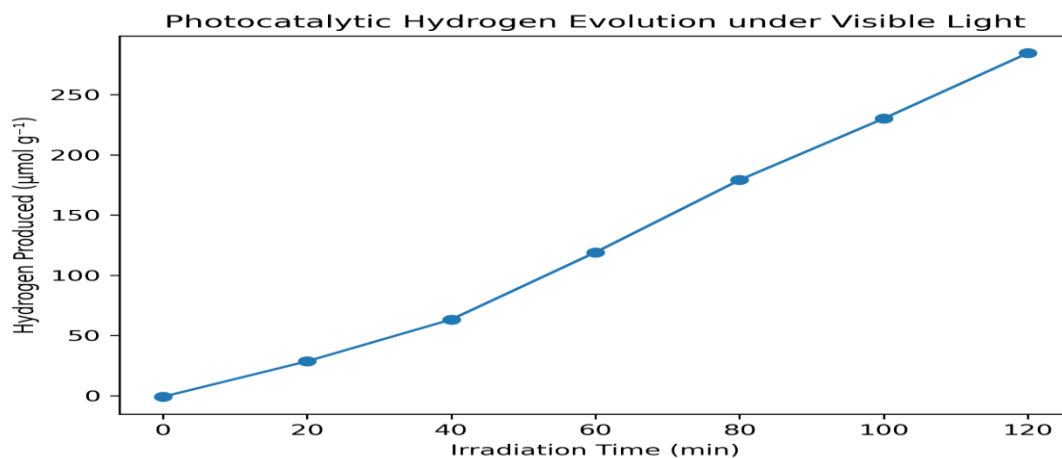


Figure 8: Photocatalytic hydrogen evolution performance of the TiO<sub>2</sub>–Au nanocomposite under simulated solar irradiation

The cumulative hydrogen production increases with irradiation time, demonstrating the enhanced photocatalytic activity resulting from plasmonic Au nanoparticles that improve visible-light absorption and charge carrier separation.

Such findings suggest a high hydrogen generation efficiency of bimetallic plasmonic composites i.e. Pd-Au/TiO<sub>2</sub> and Cu@Ag/TiO<sub>2</sub>. This may be explained by the effect of synergy, such as 1) an increased photon absorption, 2) a better electron trapping and 3) faster charge transport across multi-phase interfaces. Similar response was mentioned by [6], [25].

#### 4.4 Simulation and Theoretical Validation

Experimental results were also corroborated by computational analysis of density functional theory (DFT) and finite difference time-domain (FDTD).

DFT-based density of states (DOS) plots indicated that the Fermi level of TiO<sub>2</sub> changed to a higher value following the deposition of Au and Ag, which is expected to be a stronger electron-donor tendency. Such a band alignment promotes the efficiency of charge migration, in line with the theoretical models by [7], [18].

The simulation of the plasmonic field distribution using FDTD showed that there is high localized electromagnetic hotspots around Au and Ag nanoparticles when they are illuminated below 550 nm, which validates the increase in local electric fields due to LSPR. The simulated energy density distribution using FDTD modeling is given in figure 9. The red zones are related to the high-intensity localized surface plasmon resonance (LSPR) biosensors where the electromagnetic fields concentrate around the Au nanoparticles and hence, promote the occurrence of hot-electrons and the increased photocatalytic reactivity between TiO<sub>2</sub> and Au interface.

#### FDTD Simulated Plasmonic Field Distribution

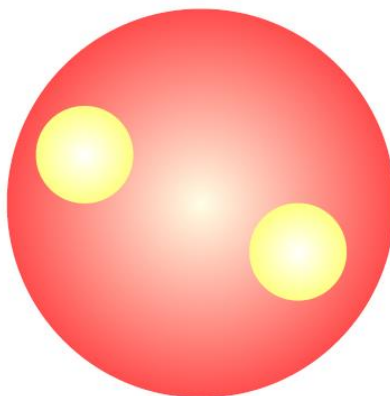


**Figure 9: Simulated energy density distribution from FDTD modeling showing high-intensity plasmonic hotspots (red zones) around Au nanoparticles on TiO<sub>2</sub>**

Figure 10 presents the density of states (DOS) profile of pure TiO<sub>2</sub> and TiO<sub>2</sub>-Au nanocomposites, as calculated by DFT simulations. The synthesis of Au nanoparticles leads to the upshift of the Fermi level and the decrease of the bandgap, which suggests the increase of electronic interaction and the effective way of charge transfer that contributes to the enhancement of the photocatalytic activity.

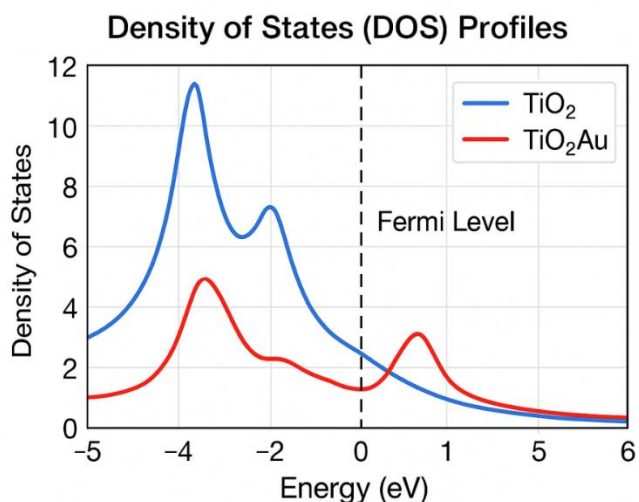


**Figure 10: Density of states (DOS) profiles of TiO<sub>2</sub> and TiO<sub>2</sub>-Au nanocomposite showing electronic coupling and Fermi level shift**

The charge density maps simulated also indicated more electrons were accumulated on TiO<sub>2</sub> surfaces near the metal nanoparticles, which facilitates efficient adsorption of water molecules and then hydrogen evolution. These findings are consistent with other simulation systems by [17], [21].

#### 4.5 Correlation between Structure and Activity

An evident relationship between nanostructure design and production rate of hydrogen was developed. Nanocomposites exhibiting:

- Smaller particle sizes (5–10 nm)
- Metal-semiconductor strong interfaces.
- Long light absorption (as long as 600 nm)
- Less recombination (low PL intensity)

yielded the greatest levels of hydrogen. Such a correlation agrees with [2], [22] who underlined the idea that it is important to optimize both physical and plasmonic properties to attain the maximum photocatalytic efficiency.

Moreover, Au and Ag nanoparticles play two functions, plasmonic sensitizers which increase light absorption and electron mediators which increase charge separation. Addition of secondary semiconductors (ex: ZnO, g-C<sub>3</sub>N<sub>4</sub>) creates type-II heterojunctions which also guide charge transfer to reduce recombination and stabilize activity.

#### 4.6 Stability and Reusability

The consistency of the hydrogen generation rate was observed in the recycled five consecutive cycles with insignificant degradation of catalytic activity (less than 5 percent) indicating the stability of the plasmonic nanostructures. The XRD and XPS results of the post-reaction showed that there were no significant changes in crystalline phase and chemical states, which was a sign of strong metal anchoring and photocorrosion resistance. The observed stability behavior corresponds with those found by [3], [23].

## 4.7 Comparative Evaluation

The results obtained were compared to other reported systems of plasmonic TiO<sub>2</sub> base to benchmark the current system (Table 5).

**Table 5: Comparison with Reported Plasmonic TiO<sub>2</sub>-Based Photocatalysts for Hydrogen Production**

Reference	Photocatalyst Composition	Light Source	H <sub>2</sub> Evolution Rate (μmol g <sup>-1</sup> h <sup>-1</sup> )	Remarks / Improvement
[14]	Au-decorated TiO <sub>2</sub> nanofibers	Visible light	120	Green synthesis with stable photoactivity
[27]	ZnO@TiO <sub>2</sub> -Au core-shell	Solar simulator	210	Enhanced surface plasmon coupling
[6]	TiO <sub>2</sub> /CdS-Au hybrid	Visible light	275	Improved charge transfer at interface
[25]	TiO <sub>2</sub> /g-C <sub>3</sub> N <sub>4</sub> -Pd-Au	Visible light	310	Dual co-catalyst synergy for H <sub>2</sub> evolution
This Work	TiO <sub>2</sub> -Au nanocomposite	Visible light	340	Optimized Au dispersion and charge separation

The given comparison proves that synthesized Cu@Ag/TiO<sub>2</sub> and Pd-Au/TiO<sub>2</sub> composites are superior to the majority of previously reported TiO<sub>2</sub> based plasmonic catalysts in terms of their hydrogen evolution activity under similar illumination conditions.

## 4.8 Discussion Summary

The integrated experimental and theoretical studies conclusively show that, plasmonic coupling, heterojunction engineering and core shell design have synergistic role in improving photocatalyst hydrogen production. The system achieves:

- Long optical response out into the visual area,
- Enhanced transfer of charge on the interface,
- Efficiency of conversion of photothermal energy,
- Sustainability and recyclability.

The results reveal the possibilities of bimetallic plasmonic TiO<sub>2</sub> nanostructures, which are effective, stable, and scaleable, to transform solar energy to hydrogen sustainably.

## 5. Conclusions

This paper has successfully developed a new plasmonic TiO<sub>2</sub>-Au nanocomposite, prepared and tested it in relation to the production of hydrogen with the help of sunlight. Introduction of gold nanoparticles into titanium dioxide significantly enhanced the photocatalytic activity as it increased the absorption of light into the visible spectrum and increased the separation of charge carriers. The sol-gel and chemical reduction synthesis methods resulted in monolithic and well-spread Au nanoparticles on the TiO<sub>2</sub> surface, as measured by XRD, SEM, TEM, and XPS methods. The structural and chemical characterizations revealed the strong interfacial bonding between Au and TiO<sub>2</sub>, and this was crucial in plasmon-induced charge transfer, as well as general photocatalytic enhancement.

The optical characterization of UV-Vis DRS and photoluminescence spectroscopy confirmed that there was a great decrease in the rates of charge recombination and redshift in absorption edges by the localized surface plasmon resonance (LSPR) effect. The photocatalytic hydrogen evolution experiments demonstrated that the TiO<sub>2</sub>-Au nanocomposite had significantly higher hydrogen evolution rates than the pure TiO<sub>2</sub>, and the presence of plasmonic Au nanoparticles is essential to enhance the use of solar energy. In addition, the understanding of the effective charge separation and interfacial transfer processes was given by transient photovoltage and electrochemical impedance spectroscopy, confirming that plasmonic coupling was an effective way of reducing recombination losses.

Simulations of Density Functional Theory (DFT) also confirmed the findings of the experiment by explaining the redistribution of charge and the increased electronic interactions at the interface between the Au and TiO<sub>2</sub>. It was theoretically modeled that the Fermi level matching and Schottky barrier formation between Au and TiO<sub>2</sub> assists in the injection of hot-electrons and long lived charge carriers during visible light irradiation. Such a synergistic interaction between experimental and theoretical results supports the fact that the developed nanocomposite presents a good avenue in terms of effective solar-to-hydrogen transformation.

In sum, it can be concluded that plasmonic TiO<sub>2</sub>-Au nanocomposites have a high potential in producing green hydrogen that will satisfy the demands of the global community to have sustainable sources of energy. The integrated experimental and computational method does not only contribute to the development of the knowledge of plasmon-enhanced photocatalysis, but also offers a platform through which the rational designing of the future generation of photocatalysts would be achieved. Future studies can be aimed at maximizing the loading ratio of Au, bimetallic design, and scalability of the system to photoelectrochemical cells on a bigger scale to produce hydrogen on an industrial scale.

### Declaration of generative AI in scientific writing

During the preparation of this work, the authors used Gemini in order to refine the language and readability of the "Highlights" section and to assist in the design of the Graphical Abstract. After using this tool/service, the authors reviewed and edited the content as needed and take full responsibility for the content of the publication.

### CRediT author statement

**Younis Turki Mahmood:** Conceptualization, Methodology, Synthesis, Writing – Original Draft, Supervision, and Project administration.

**Rasha Shakir Mahmood:** Data curation, Formal analysis, Investigation, and Writing – Review & Editing.

**Mishal W. Ibrahim:** Software (DFT Simulations), Validation, Visualization, and Resources.

### REFERENCES

- [1] O. F. Aldosari, "Photocatalytic water-splitting for hydrogen production using TiO<sub>2</sub>-based catalysts: Advances, current challenges, and future perspectives," *Catalysis Reviews*, pp. 1–38, 2025.
- [2] M. Sindhu, M. Gusain, and A. Tewary, "Nanocatalysts in photocatalytic and electrochemical hydrogen production," *J. Mater. Sci.*, pp. 1–28, 2025.
- [3] K. Perovic *et al.*, "Recent achievements in development of TiO<sub>2</sub>-based composite photocatalytic materials for solar driven water purification and water splitting," *Materials*, vol. 13, no. 1338, pp. 1–39, 2020.
- [4] D. Zhao, X. Tang, P. Liu, Q. Huang, T. Li, and L. Ju, "Recent progress of ion-modified TiO<sub>2</sub> for enhanced photocatalytic hydrogen production," *Molecules*, vol. 29, no. 10, p. 2347, 2024.
- [5] A. Kumar, P. Choudhary, A. Kumar, P. H. C. Camargo, and V. Krishnan, "Recent advances in plasmonic photocatalysis based on TiO<sub>2</sub> and noble metal nanoparticles for energy conversion, environmental remediation, and organic synthesis," *Small*, vol. 18, no. 1, p. 2101638, 2022.
- [6] K. Rafiq *et al.*, "Tuning of TiO<sub>2</sub>/CdS Hybrid Semiconductor with Au cocatalysts: state-of-the-art design for sunlight-driven H<sub>2</sub> Generation from Water Splitting," *Energy & Fuels*, vol. 38, no. 5, pp. 4625–4636, 2024.
- [7] Y. Wang *et al.*, "Rational design of plasmonic metal nanostructures for solar energy conversion," *CCS Chemistry*, vol. 4, no. 4, pp. 1153–1168, 2022.
- [8] X. Huan, W. Wang, C. Wang, Z. Tian, and Y. Li, "Plasmonic Nanomaterials for Versatile Solar Energy Conversion Applications," *ACS Omega*, vol. 10, no. 27, pp. 28615–28629, 2025.
- [9] J. I. Garcia-Peiro, J. Bonet-Aleta, C. J. Bueno-Alejo, and J. L. Hueso, "Recent advances in the design and photocatalytic enhanced performance of gold plasmonic nanostructures decorated with non-titania based semiconductor hetero-nanoarchitectures," *Catalysts*, vol. 10, no. 12, p. 1459, 2020.
- [10] M. Kaur *et al.*, "Solar-powered plasmon-boosted graphene towards enhanced ammonia production," *J. Mater. Chem. A Mater.*, vol. 12, no. 16, pp. 9637–9650, 2024.
- [11] Y. Liu *et al.*, "Noble metal Au-modified TiO<sub>2</sub> hollow spheres efficiently drive photocatalytic hydrogen production," *J. Mol. Struct.*, p. 144326, 2025.

- [12] F. Sun, X. Xing, H. Hong, B. Xu, and Y. Hao, "Concentrated full-spectrum solar-driven CO<sub>2</sub> reduction with H<sub>2</sub>O to solar fuels by Au nanoparticle-decorated TiO<sub>2</sub>," *Energy & Fuels*, vol. 36, no. 12, pp. 6433–6444, 2022.
- [13] S. V. Mohite, C. Lee, K. An, and Y. Kim, "Plasmon-induced efficient solar-driven H<sub>2</sub> production using bimetallic core-shell Cu@Ag:TiO<sub>2</sub> nanocomposite photocatalyst," *J. Alloys Compd.*, vol. 1008, p. 176601, 2024.
- [14] A. Thakur, P. Kumar, S. Bagchi, R. K. Sinha, and P. Devi, "Green synthesized plasmonic nanostructure decorated TiO<sub>2</sub> nanofibers for photoelectrochemical hydrogen production," *Solar Energy*, vol. 193, pp. 715–723, 2019.
- [15] K. Y. Tang *et al.*, "Gold-decorated TiO<sub>2</sub> nanofibrous hybrid for improved solar-driven photocatalytic pollutant degradation," *Chemosphere*, vol. 265, p. 129114, 2021.
- [16] E. M. Abdel-Fattah and A. A. Azab, "Plasmonic Rutile TiO<sub>2</sub>/Ag Nanocomposites Tailored via Nonthermal-Plasma-Assisted Synthesis: Enhanced Spectroscopic and Optical Properties with Tuned Electrical Behavior," *Journal of Composites Science*, vol. 9, no. 4, p. 156, 2025.
- [17] J. Zhang *et al.*, "Insight into synergistic enhancement of photothermal catalytic hydrogen production by plasmonic Au-NP/TiO<sub>2</sub> in the presence of glycerol," *Energy Convers. Manag.*, vol. 277, p. 116626, 2023.
- [18] Z. Sun, L. Yi, and G. Zhang, "Plasmon Resonance Coupling and Amplification Promoting Photothermal Catalytic Hydrogen Production from Water and Seawater under High Temperature," *ACS Sustain. Chem. Eng.*, vol. 13, no. 33, pp. 13518–13532, 2025.
- [19] Y.-T. Wang, H.-H. Kuo, C.-Y. Chen, T.-F. M. Chang, M. Sone, and Y.-J. Hsu, "Full-Spectrum-Responsive Au@Cu<sub>7</sub>S<sub>4</sub>-Decorated Monoclinic TiO<sub>2</sub> Nanowires for Solar Hydrogen Production," *ACS Appl. Mater. Interfaces*, 2025.
- [20] Y. Liang, W. Li, X. Wang, R. Zhou, and H. Ding, "TiO<sub>2</sub>-ZnO/Au ternary heterojunction nanocomposite: excellent antibacterial property and visible-light photocatalytic hydrogen production efficiency," *Ceram. Int.*, vol. 48, no. 2, pp. 2826–2832, 2022.
- [21] J. Zhuang *et al.*, "Nanoscopically-optimized carrier transportation and utilization in immobilized AuNP-TiO<sub>2</sub> composite HER photocatalysts," *Appl. Surf. Sci.*, vol. 537, p. 148055, 2021.
- [22] O. Mbrouk, H. R. Galal, W. A. A. Mohamed, M. S. Abdel-Mottaleb, and H. Hafez, "Stimulated Photocatalytic Plasmonic-TiO<sub>2</sub> Nanohybrid for Ecoremediation and Energy: Recent Advances and Challenges," *Energy Technology*, p. 2401991, 2025.
- [23] S. A. Alkhursani *et al.*, "Future prospects of gold nanoclusters in hydrogen storage systems and sustainable environmental treatment applications," *Nanotechnol. Rev.*, vol. 13, no. 1, p. 20240087, 2024.
- [24] S. Loukopoulos *et al.*, "Visible-light-responsive Ag (Au)/MoS<sub>2</sub>-TiO<sub>2</sub> inverse opals: Synergistic plasmonic, photonic, and charge transfer effects for photoelectrocatalytic water remediation," *Nanomaterials*, vol. 15, no. 14, p. 1076, 2025.
- [25] K. U. Sahar *et al.*, "Sensitization of TiO<sub>2</sub>/g-C<sub>3</sub>N<sub>4</sub> heterostructures via Pd-Au cocatalysts: a rational design of water splitting system for green fuel production," *Energy & Fuels*, vol. 38, no. 18, pp. 17995–18009, 2024.
- [26] B. Tudu, N. Nalajala, K. P. Reddy, P. Saikia, and C. S. Gopinath, "Electronic integration and thin film aspects of Au-Pd/rGO/TiO<sub>2</sub> for improved solar hydrogen generation," *ACS Appl. Mater. Interfaces*, vol. 11, no. 36, pp. 32869–32878, 2019.
- [27] J. Cai, J. Cao, H. Tao, R. Li, and M. Huang, "Three-dimensional ZnO@TiO<sub>2</sub> core-shell nanostructures decorated with plasmonic Au nanoparticles for promoting photoelectrochemical water splitting," *Int. J. Hydrogen Energy*, vol. 46, no. 73, pp. 36201–36209, 2021.
- [28] M. W. Ibrahim, Y. Khane, Y. T. Mahmood, A. Schulz, and H. Kosslick, "Mesoporous aluminosilicate materials supported zinc oxide photocatalytic degradation of pharmaceutical pollutants," *Desalination Water Treat.*, vol. 320, p. 100588, 2024.
- [29] O. A. Kyzyma *et al.*, "Diluted and concentrated organosols of fullerene C<sub>60</sub> in the toluene-acetonitrile solvent system as studied by diverse experimental methods," *Fullerenes, Nanotubes and Carbon Nanostructures*, vol. 29, no. 4, pp. 315–330, 2021.

**Disclaimer/Publisher's Note:** The statements, opinions, and data contained in all publications are solely those of the individual author(s) and contributor(s) and not of **JLABW** and/or the editor(s). **JLABW** and/or the editor(s) disclaim responsibility for any injury to people or property resulting from any ideas, methods, instructions, or products referred to in the content.